Chapter 2
HEV Modeling

2.1 Introduction

The objective of the energy management control is to minimize the vehicle fuel consumption, while maintaining the battery state of charge around a desired value. To this end, modeling for energy management may have two scopes: creating plant simulators to which an energy management strategy is applied for testing and development, or creating embedded models that are used to set up analytically and/or solve numerically the energy management problem. Plant models tend to be more accurate and computationally heavy than embedded control models. The main objective in both cases is to reproduce the energy flows within the powertrain and the vehicle, in order to obtain an accurate estimation of fuel consumption and battery state of charge, based on the control inputs and the road load. In some applications, other quantities may be of interest, such as thermal flows (temperature variation in engine, batteries, after-treatment, etc.), battery aging, pollutant emissions, etc.

This chapter provides a concise overview of the modeling issues linked to the development and simulation of energy management strategies. The reader is referred to more specialized works for further details (e.g., [1]). Efficiency considerations are at the basis of the models described, which are suited for preliminary analysis and high-level energy management development.

2.2 Modeling for Energy Analysis

Because of the losses in the powertrain, the net amount of energy produced at the wheels is smaller than the amount of energy introduced into the vehicle from external sources (e.g., fuel). Conversion losses take place when power is transformed into a different form (e.g., chemical into mechanical, mechanical into electrical, etc.). Similarly, when power flows through a connection device, friction losses and other inefficiencies reduce the amount of power at the device output. Energy losses in powertrain components are usually modeled using efficiency maps, i.e., tables that contain efficiency data as a function of the operating conditions (for example, the output torque and the rotational speed of the engine). Maps are built experimentally

S. Onori et al., *Hybrid Electric Vehicles*, SpringerBriefs in Control, Automation and Robotics, DOI 10.1007/978-1-4471-6781-5_2

as a set of stationary points, i.e., letting the component reach a steady-state operating condition and measuring power input and output (and/or power dissipation) in that condition. Because of this procedure, efficiency maps may not be accurate during transients. Despite this, the approach is widely used because it allows to generate simple models capable of being evaluated quickly when implemented in computer code, and validation results [2] show that the accuracy of such models can be very good for estimating fuel consumption and energy balance, as most of the energy content is associated with the slower system dynamics [3].

The vehicle fuel consumption for a prescribed driving cycle can be estimated using a *backward* or a *forward* modeling approach. The backward, quasi-static approach is based on the assumption that the prescribed driving cycle is followed exactly by the vehicle. The driving cycle is subdivided in small time intervals, during which an average operating point approach is applied, assuming that speed, torque, and acceleration remain constant: this is equivalent to neglecting internal powertrain dynamics and taking average values of all variables during the selected sampling time, which is therefore longer than typical powertrain transients (e.g., engine dynamics, gear shifting), and of the same order of magnitude of vehicle longitudinal dynamics and driving cycle variations. Each powertrain component is modeled using an efficiency map, a power loss map, or a fuel consumption map: these give a relation between the losses in the component and the present operating conditions (averaged during the desired time interval).

The forward, dynamic approach is based on a first-principles description of each powertrain component, with dynamic equations describing the evolution of its state. The degree of modeling detail depends on the timescale and the nature of the phenomena that the model should predict. In the simplest case, the same level of detail as the quasi-static approach can be applied, but the evolution of vehicle speed is computed as the result of the dynamic simulation and not prescribed a priori.

2.3 Vehicle-Level Energy Analysis

By vehicle-level energy analysis, we refer to the case in which the vehicle is considered as a point mass and its interaction with the external environment is studied, in order to compute the amount of power and energy needed to move it with specified speed. This high-level approach is useful to develop an understanding of the vehicle longitudinal dynamics and of the energy characteristics of hybrid vehicles.

2.3.1 Equations of Motion

If a vehicle is considered as a mass point, its motion equation can be written from the equilibrium of forces shown in Fig. 2.1:

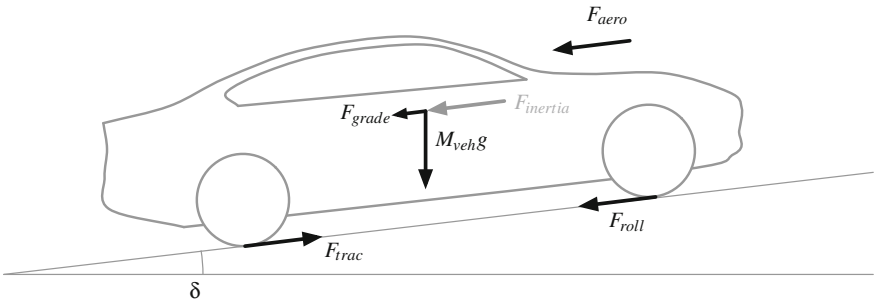

Fig. 2.1 Forces acting on a vehicle

$$M_{veh}\frac{dv_{veh}}{dt} = F_{inertia} = F_{trac} - F_{roll} - F_{aero} - F_{grade}, \tag{2.1}$$

where M_{veh} is the effective vehicle mass, v_{veh} is the longitudinal vehicle velocity, $F_{inertia}$ is the inertial force, $F_{trac} = F_{pwt} - F_{brake}$ is the tractive force generated by the powertrain and the brakes at the wheels,[1] F_{roll} is the rolling resistance (friction due to tire deformation and losses), F_{aero} the aerodynamic resistance, F_{grade} the force due to road slope.

The aerodynamic resistance is expressed as

$$F_{aero} = \frac{1}{2}\rho_{air}A_f C_d v_{veh}^2, \tag{2.2}$$

where ρ_{air} is the air density (1.25 kg/m^3 in normal conditions), A_f the vehicle frontal area, C_d the aerodynamic drag coefficient.

The rolling resistance force is usually modeled as [1]

$$F_{roll} = c_{roll}(v_{veh}, p_{tire}, \ldots)M_{veh}\mathrm{g}\cos\delta, \tag{2.3}$$

where g is the gravity acceleration, δ the road slope angle (so that $M_{veh}\mathrm{g}\cos\delta$ is the vertical component of the vehicle weight), and c_{roll} is a rolling resistance coefficient which is, in principle, a function of vehicle speed, tire pressure p_{tire}, external temperature, etc. In most cases, c_{roll} is assumed to be constant, or to be an affine function of the vehicle speed:

$$c_{roll} = c_{r0} + c_{r1}v_{veh}. \tag{2.4}$$

[1] This is the sum of the forces acting on the individual wheels. For each wheel, it represents the net torque acting on the wheel divided by the effective tire radius. Note that the tire radius is assumed here to be equal to the nominal tire radius, but it can be very different from this value during dynamic transient maneuvers, which are not considered in this book. See a vehicle dynamics textbook for more details on the modeling of ground/tire forces (see, e.g., [4]).

Table 2.1 Typical values of vehicle-dependent parameters for longitudinal vehicle dynamics models

Parameter	Compact car	Full-size car	SUV
M_{veh}	1200–1500 kg	1700–2000 kg	1900–2200 kg
C_d	0.3–0.35	0.28–0.33	0.32–0.38
A_f	1.3–1.7 m^2	1.8–2.2 m^2	2–2.5 m^2
c_{roll}	0.01–0.03	0.01–0.03	0.01–0.03

The order of magnitude of c_{roll} is 0.01–0.03 (for a light vehicle on normal road surface), which means that the rolling resistance is 1–3 % of the vehicle weight (depending on vehicle, soil, tires and tire pressure, temperature, etc.).

The grade force is the horizontal component of the vehicle weight, which opposes (or facilitates) vehicle motion only if the vehicle is moving uphill (or downhill):

$$F_{grade} = M_{veh} g \sin \delta. \tag{2.5}$$

These basic equations represent the starting point for vehicle modeling, and can be sufficiently accurate if the parameters are correctly identified. Typical values of the vehicle-level parameters are listed in Table 2.1.

2.3.2 Forward and Backward Modeling Approaches

Equation (2.1) can be rearranged to calculate the tractive force that the powertrain needs to produce, given the acceleration (inertial force $F_{inertia}$):

$$F_{trac} = F_{pwt} - F_{brake} = F_{inertia} + F_{grade} + F_{roll} + F_{aero}. \tag{2.6}$$

The different form of (2.1) and (2.6) corresponds to the forward and backward modeling approaches: in (2.1), the vehicle acceleration $\frac{dv_{veh}}{dt}$ is computed as a consequence of the tractive force generated by the powertrain (and obviously the external resistance terms), and the speed is then obtained by integration of the acceleration; this is the *forward* approach, which reproduces the physical causality of the system. On the other hand, in the *backward* approach modeled by (2.6), force follows velocity and the tractive force is calculated starting from the inertia force: in this case, it is assumed that the vehicle is following a prescribed velocity (and acceleration) profile, and F_{trac} represents the corresponding force that the powertrain must supply.

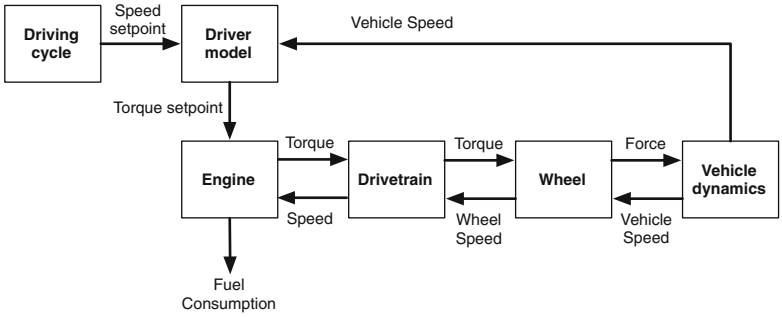

Fig. 2.2 Information flow in a forward simulator

The forward approach is the option typically chosen in most simulators; it is characterized by the information flow as shown in Fig. 2.2. For example, in the case of a hybrid vehicle forward simulator, the desired speed (from the cycle inputs) is compared to the actual vehicle speed, and braking or throttle commands are generated using a driver model (e.g., a PID speed controller) in order to follow the imposed vehicle profile. This driver command is an input to the supervisor block that is responsible of issuing the actuators setpoints (engine, electric machines, and braking torques) to the rest of the powertrain components, which ultimately produce a tractive force. Finally, the force is applied to the vehicle dynamics model, where the acceleration is determined with (2.1), taking into account the road load information [5].

In a backward simulator, instead (see Fig. 2.3), no driver model is necessary, since the desired speed is a direct input to the simulator, while the engine torque and fuel consumption are outputs. The simulator determines the net tractive force to be applied based on the velocity, payload, and grade profiles, along with the vehicle characteristics. Based on this information, the torque that the powertrain should apply is calculated, and then the torque/speed characteristics of the various powertrain components are taken into account in order to determine the engine operating conditions and, finally, the fuel consumption.

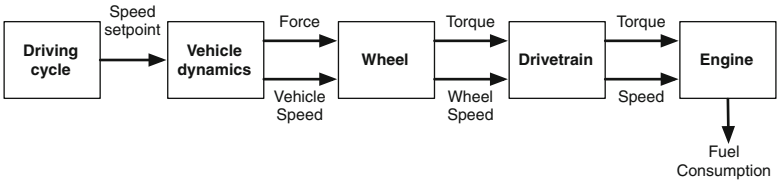

Fig. 2.3 Information flow in a backward simulator

Both the forward and backward simulation approaches have their relative strengths and weaknesses. Fuel economy simulations are typically conducted over predetermined driving cycles, and therefore using a backward simulator ensures that each different simulation exactly follows this profile, which guarantees consistency of simulation results. By contrast, a forward simulator may not exactly follow the trace, as it introduces a small error between the actual and the desired signal. Proper tuning of the driver block can reduce the differences, whereas the backward version keeps the error at zero without any effort. On the other hand, a backward simulation assumes that the vehicle and powertrain are capable of following the speed trace, and does not account for limitations of the powertrain actuators in computing the vehicle speed, which is predetermined. This poses the problem of evaluating demanding cycles which may require more power than the powertrain can provide. A forward simulation does not have this issue, because the speed is computed from the torque/force output, which can be saturated according to the powertrain limitations. For this reason, forward simulation can also be used for acceleration tests and in general for testing the behavior of the system at saturation. In addition, forward simulators are implemented according to physical causality and, if their level of detail is appropriate, can be used for development of online control strategies, while a backward simulator is suited for preliminary screening of energy management strategies. It is possible to combine the advantages of both modeling approaches, i.e., the accurate reproduction of a cycle by a backward simulation and the ability to capture powertrain limitations of a forward simulator. A solution, represented in Fig. 2.4, consists in using a forward simulator in which the driver model (speed controller) uses a backward vehicle model to compute the torque setpoints to be applied: in this way, the resulting speed profile will match exactly the reference cycle, if this does not

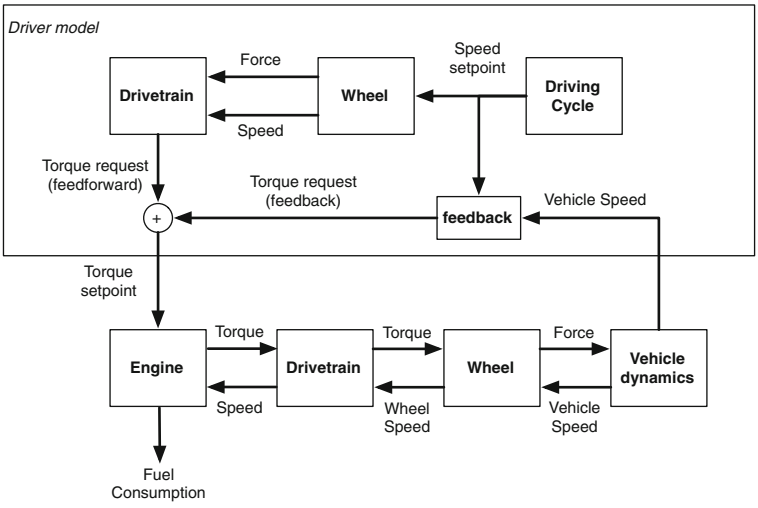

Fig. 2.4 Information flow in a backward–forward simulator

saturate the powertrain capacity, but will be appropriately saturated when needed since it goes through a forward powertrain model. A feedback term should also be added, in order to recover speed deviation due to powertrain saturation (or to possible mismatches between the backward and forward models).

2.3.3 Vehicle Energy Balance

Fuel consumption evaluation is conducted by analyzing the energy flows in the powertrain and identifying the areas in which saving can be introduced. From (2.6) the inertial force $F_{inertia}$ is positive when the vehicle is accelerating, and negative during deceleration; the grade force F_{grade} is positive when the vehicle is driven uphill and negative when it is going downhill; the rolling (F_{roll}) and aerodynamic (F_{aero}) resistances are always positive (for a vehicle moving in forward direction).

The forces F_{roll} and F_{aero} are dissipative, since they always oppose the motion of the vehicle, while the inertial and grade forces are conservative, being only dependent on the vehicle state (respectively velocity and altitude). Thus, part of the tractive force generated by the powertrain increases the kinetic and potential energy of the vehicle (by accelerating it and moving it uphill), and part is dissipated in rolling and aerodynamic resistances. When the vehicle decelerates or drives downhill, its potential and kinetic energy must be dissipated: rolling and aerodynamic resistances contribute to dissipating part of the vehicle energy, but for faster deceleration the mechanical brakes must be used. Thus, ultimately, all the energy that the powertrain produces is dissipated in these three forms: rolling resistance, aerodynamic resistance, and mechanical brakes. The net variation of kinetic energy is always zero between two stops (since initial speed and final speed are both zero), and the variation of potential energy only depends on the difference of altitude between the initial and ending point of the trip considered.

Multiplying all terms of (2.6) by the vehicle speed (v_{veh}) the following balance of power is obtained:

$$P_{trac} = P_{inertia} + P_{grade} + P_{roll} + P_{aero}. \tag{2.7}$$

The term P_{trac} represents the tractive power at the wheels, either positive or negative. Positive P_{trac} is generated by the powertrain to propel the vehicle, while negative P_{trac} (corresponding to deceleration) can be obtained using the powertrain, the brakes or both. In conventional vehicles, the amount of negative power that the powertrain can absorb is rather limited: it consists in friction losses in the various components and pumping losses in the engine. In hybrid electric vehicles, the amount of negative power is much higher, since the electric traction machines are reversible and can be used for deceleration as well as acceleration.

The term $P_{inertia} = M_{veh}\dot{v}_{veh}v_{veh}$ represents the amount of power needed just to accelerate the vehicle (without considering the losses); the terms $P_{roll} = F_{roll}v_{veh}$ and $P_{aero} = F_{aero}v_{veh}$ are the amount of power needed to overcome the rolling and

aerodynamic resistances respectively; and $P_{grade} = F_{grade} v_{veh}$ is the power that goes into overcoming a slope (or, if the slope is negative and the vehicle is going downhill, it is the power that accelerates the vehicle and, when excessive, must be dissipated to prevent undesired acceleration).

If the terms that appear in (2.7) are integrated over the duration of a trip (time interval $[t_0\ t_f]$), the following energy balance is obtained:

$$E_{trac} = \int_{t_0}^{t_f} P_{trac} dt = E_{kin} + E_{pot} + E_{roll} + E_{aero}, \tag{2.8}$$

where the individual terms are:

$$E_{kin} = \int_{t_0}^{t_f} P_{inertia} dt = M_{veh} \int_{t_0}^{t_f} v_{veh}(t) \dot{v}_{veh}(t) dt; \tag{2.9a}$$

$$E_{pot} = \int_{t_0}^{t_f} P_{grade} dt = M_{veh} \mathrm{g} \int_{t_0}^{t_f} v_{veh}(t) \sin \delta(t) dt; \tag{2.9b}$$

$$E_{roll} = \int_{t_0}^{t_f} P_{roll} dt = M_{veh} \mathrm{g} \int_{t_0}^{t_f} c_{roll} v_{veh}(t) \cos \delta(t) dt; \tag{2.9c}$$

$$E_{aero} = \int_{t_0}^{t_f} P_{aero} dt = \frac{1}{2} \rho_{air} A_f C_d \int_{t_0}^{t_f} v_{veh}(t)^3 dt. \tag{2.9d}$$

Note that the integral of the inertial power $P_{inertia}$ is the variation of kinetic energy E_{kin}, and the integral of the grade power P_{grade} is the variation of potential energy E_{pot}. Each energy term is the product of two terms: one representing vehicle parameters (mass, resistance coefficients), which are independent of the driving cycle, and the other representing driving cycle information, independent of the vehicle characteristics and only function of the velocity profile[2] $v_{veh}(t)$.

The relative amount of rolling resistance, aerodynamic resistance, and brake energy defines the characteristics of a driving cycle. In particular, the potential for energy recovery using regenerative braking is equal to the amount of kinetic and potential energy that needs to be dissipated, minus the quantity that is dissipated because of rolling and aerodynamic resistance. Thus, a urban driving cycle with frequent accelerations and decelerations at low speed (where the resistances are lower) presents more potential for energy recovery than a highway cycle in which the speed is approximately constant and the losses due to aerodynamic resistance represent the major component of the power requested by the vehicle.

To better understand this concept, it is useful to look separately at the energy balance during acceleration ($\dot{v}_{veh} \geq 0$) and deceleration ($\dot{v}_{veh} < 0$), i.e., compute the integrals above by summing over different sections of the driving cycle. Let us denote with the superscript $^+$ the energy values computed by considering only the instants in which $\dot{v}_{veh} \geq 0$, and with the superscript $^-$ those relative to the instants in

[2] An exception is the rolling resistance contribution E_{roll}, because the coefficient c_{roll} may, in general, depend on vehicle speed as well as vehicle and tire characteristics.

which $\dot{v}_{veh} < 0$ (i.e., the integrals (2.9a, 2.9b, 2.9c, 2.9d) are split into two domains, according to the sign of $\dot{v}_{veh}$).

The kinetic energy in the two cases is equal, but with opposite sign:

$$E_{kin}^{-} = -E_{kin}^{+} \tag{2.10}$$

because the net variation of kinetic energy is zero during the entire cycle, and its variation is positive each time $\dot{v}_{veh} > 0$, and negative each time that $\dot{v}_{veh} < 0$.

The amount of energy that the powertrain must deliver during acceleration is thus:

$$E_{pwt}^{+} = E_{roll}^{+} + E_{aero}^{+} + E_{pot}^{+} + E_{kin}^{+}, \tag{2.11}$$

that is, the energy provided by the powertrain is spent to: accelerate the vehicle (increase its kinetic energy by E_{kin}^{+}); move it at a higher level (E_{pot}^{+}); and overcome dissipative resistances (E_{roll}^{+} and E_{aero}^{+}). However, in the course of a complete trip (vehicle starting from standstill and coming to a stop at the end), the net variation of kinetic energy is zero. Therefore, the same amount of kinetic energy produced during acceleration (E_{kin}^{+}) must be removed from the vehicle during deceleration.

When the vehicle decelerates, it needs to dissipate the entire amount of kinetic energy accumulated during acceleration. The dissipative resistances contribute to this, since they tend to slow down the vehicle. However, the amount of kinetic energy to dissipate during deceleration may be higher than the sum of rolling and aerodynamic resistance; in this case, the vehicle must be decelerated using additional actuators, for example using mechanical brakes or, in a hybrid vehicle, producing negative torque with electric traction motors, thus recuperating (some of) the energy. The amount of energy available for regeneration, $E_{regen,pot}$, is the total vehicle energy cumulated during acceleration (kinetic and potential) minus the losses during the deceleration phase, given by dissipative losses (rolling resistance and aerodynamic drag) and by the increase of potential energy (E_{pot}^{-})[3]:

$$E_{regen,pot} = E_{kin}^{+} + E_{pot}^{+} - E_{roll}^{-} - E_{aero}^{-} - E_{pot}^{-} \tag{2.12}$$

The diagram in Fig. 2.5 shows graphically this concept: proceeding from left to right, losses are subtracted to compute the energy available at each stage.

2.3.4 Driving Cycles

As implied in the previous section, the advantages of hybrid vehicles depend on how the vehicle is used. In particular, the hybridization advantages consist essentially in

[3] In other words, if the vehicle is decelerating uphill, part of its kinetic energy is lost to overcome the gravity; downhill, on the other hand, the gravitational force will increase the amount of energy to be regenerated.

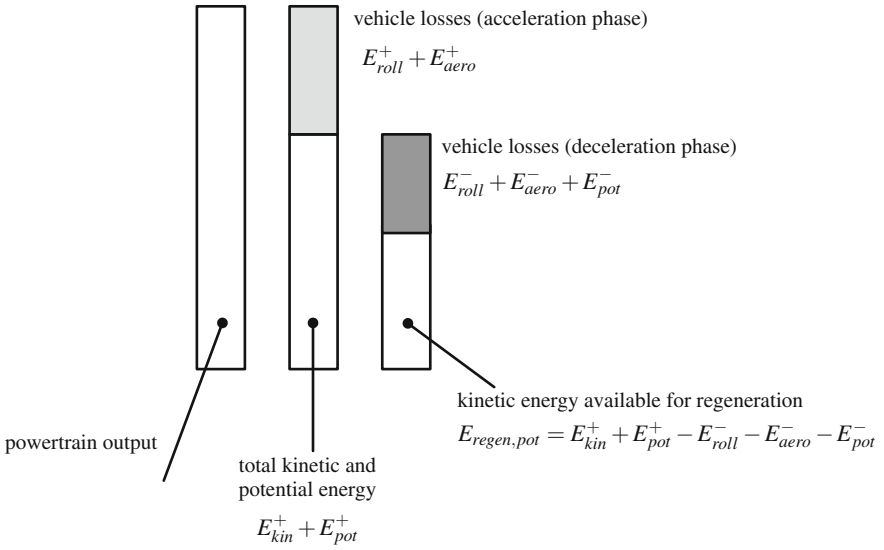

Fig. 2.5 Vehicle energy balance (bar length represents energy)

recovering potential and kinetic energy that would otherwise be dissipated in the brakes, and in operating the engine in its highest-efficiency region. If the engine had a constant efficiency and the vehicle drove at constant speed on a flat road, there would be no advantage in a hybrid electric configuration.

A *driving cycle* represents both the way the vehicle is driven during a trip and the road characteristics. In the simplest case, it is defined as a time history of vehicle speed (and therefore acceleration) and road grade. Together with the vehicle characteristics, this completely defines the road load, i.e., the force that the vehicle needs to exchange with the road during the driving cycle.

As pointed out in Sect. 2.3.3, each term in the energy balance is a function of both the driving cycle (speed, acceleration, grade) and the vehicle (mass, frontal area, coefficients of aerodynamic and rolling resistance). For this reason, the fuel consumption of a vehicle must always be specified in reference to a specific driving cycle. On the other hand, given a driving cycle, the absolute value of the road load and also the *relative* magnitude of its components depend on the vehicle characteristics.

The necessity for a standard method to evaluate emissions and fuel consumption of all vehicles on the market, and to provide a reliable basis for their comparison, led to the introduction of a reduced number of regulatory driving cycles: any vehicle sold must be tested, according to detailed procedures, using one or more of these standard cycles, which are different for each world region.

Examples of standard cycles are shown in Fig. 2.6, which also include a basic energy analysis comparison.

These driving cycles are designed to be representative of urban and extra-urban driving conditions. The Japan 10–15 and European cycle (NEDC) are synthetic,

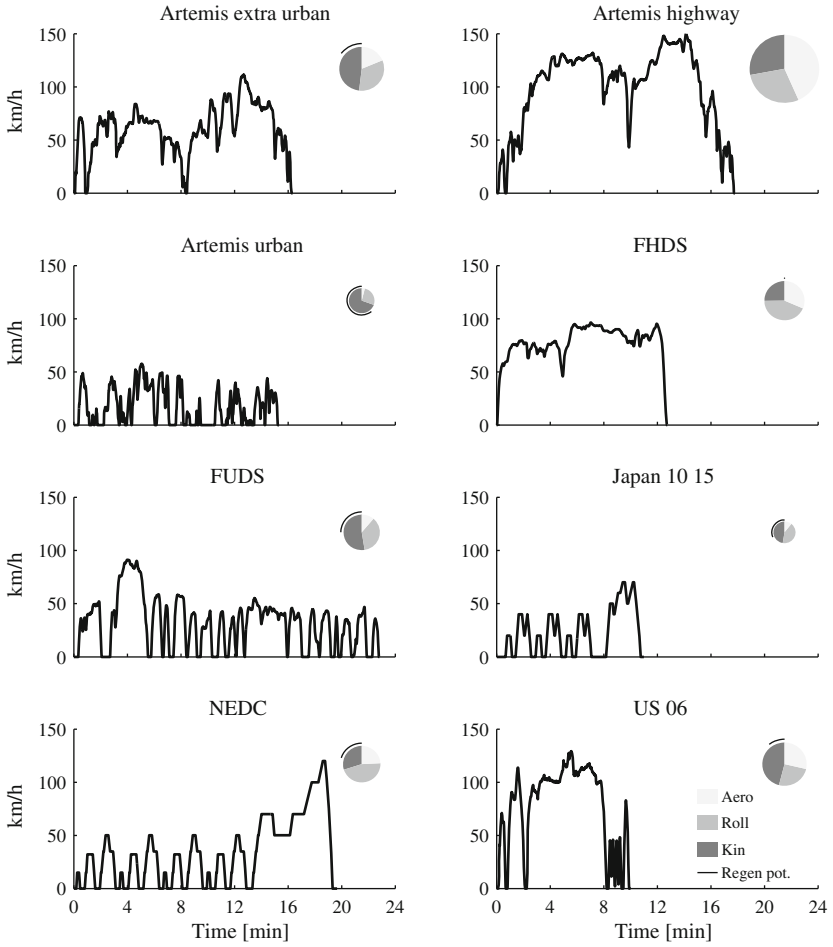

Fig. 2.6 Some examples of standard driving cycles. The pie chart shows the relative amount of the energy terms E^+_{kin}, E^+_{aero}, E^+_{roll}, as well as the amount of kinetic energy that can be recovered according to (2.12). The pie surface is proportional to the total cycle energy E^+_{pwt} defined by (2.11). Energies are computed with the vehicle data of Table 8.1

while the others reproduce measures of vehicle speed in actual roads. However, with the exception of US 06, the acceleration levels are well below the capabilities of any modern car, therefore the fuel consumption results are typically optimistic and unable to reproduce real-world driving conditions.

The regulatory cycles should be considered a standard comparison tool and not as representative of actual operating conditions. In fact, it is not possible to predict how a vehicle will be driven, since each vehicle has a different usage pattern and each

driver his or her own driving style. In order to obtain more realistic estimations of real-world fuel consumption for a specific vehicle, vehicle manufacturers may develop their own testing cycles.

2.4 Powertrain Components

This section contains a description of models of the principal powertrain components suitable for energy flow modeling, neglecting component dynamics. Detailed behavioral models accurately accounting for dynamic effect are beyond the objectives of this book and can be found in specialized works.

2.4.1 Internal Combustion Engine

The following modeling approaches can be used for an internal combustion engine, in order of increasing complexity:

1. Static map;
2. Static map and lumped-parameter dynamic model;
3. Mean-value model;
4. One-dimensional fluid-dynamic model;
5. Three-dimensional fluid-dynamic model (finite-element).

The latter two approaches are necessary only for detailed studies focused on the engine subsystem, while the first three methods can be useful in models in which the engine is seen as part of a more comprehensive system (powertrain or vehicle) and as such can be employed in energy management simulators (map models) or powertrain control strategies (map with lumped-parameter dynamics or mean-value models).

The static map approach assumes the engine to be a perfect actuator, which responds immediately to the commands; the fuel consumption is computed using a map (table) as a function of the engine speed and torque, both of which are assumed to be known. In particular, the torque is typically a control input for the engine, while the speed is a measured input and derives from the coupling to the rest of the powertrain. A curve that gives the maximum engine torque as a function of the current speed is also present in this kind of models to ensure that the torque does not exceed the limits of the engine. Figure 2.7 shows the typical engine map information with fuel consumption or iso-efficiency contours, the maximum torque curve, and the optimal operation line (OOL), i.e., the combination of torque and speed that provide the maximum efficiency for any given power output. The OOL information is often used in designing heuristic energy management strategies, as a target for the engine operating points.

The map-based model can be modified to include dynamic limitations in the torque output, i.e., a delay between the commanded torque and the actual torque generated,

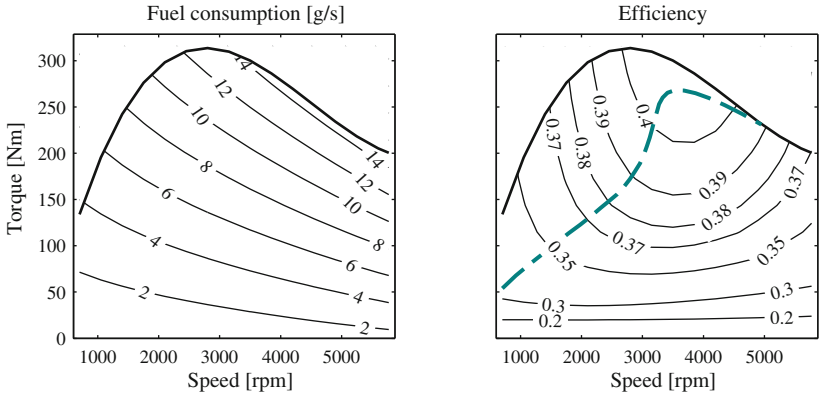

Fig. 2.7 Example of engine fuel consumption map and efficiency map (with optimal operation line, OOL, in *dashed-line*)

by coupling it to a transfer function representing air/fuel dynamics and, possibly, to an inertia representing the crankshaft dynamics.

2.4.2 Torque Converter

The torque converter is a fluid coupling device that is used to transmit motion from the engine to the transmission input shaft. It is capable of multiplying the engine torque (acting as a reduction gear), and, unlike most other mechanical joints, provides extremely high damping capabilities, since all torque is transmitted through fluid-dynamic forces rather than friction or pressure. It is traditionally used in vehicles with automatic transmissions as a launching device, because it allows for large speed differences between its two shafts while multiplying the input torque.

A torque converter (Fig. 2.8) is composed by three co-axial elements: a pump (also called impeller), connected to the engine shaft, a turbine, connected to the transmission, and a stator in between. The fluid in the torque converter is moved by

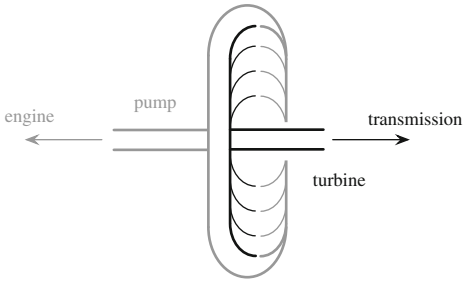

Fig. 2.8 Schematic representation of a torque converter

the pump because of engine rotation, drags the turbine, and therefore transmits torque to the transmission. The torque at the turbine is multiplied with respect to the pump torque (i.e., the engine torque), thanks to the presence of the stator which modifies the flow characteristics inside the converter. The torque multiplication increases with the speed difference between the pump and the turbine; at steady state, the two elements rotate at the same speed and the torque multiplication factor is unitary.

The torque converter model is based on tabulated characteristics of torque ratio and capacity factor versus speed ratio. The speed ratio is

$$SR = \frac{\omega_t}{\omega_p}, \tag{2.13}$$

where ω_t is the turbine speed and ω_p the pump speed. The torque ratio or multiplication ratio is

$$MR = \frac{T_t}{T_p}, \tag{2.14}$$

with T_t and T_p the turbine and pump torque respectively. The capacity factor, which is a measure of how much torque the torque converter can transmit, is defined as

$$K_{tc} = \frac{\omega_p}{\sqrt{T_p}}. \tag{2.15}$$

As an alternative to the capacity factor, the torque at 2000 rpm (MP_{2000}) is sometimes used to characterize the torque capacity; it is related to the capacity factor as follows:

$$MP_{2000} = \frac{2000^2}{K_{tc}^2}, \tag{2.16}$$

where K_{tc} must be expressed in units of $\frac{\text{RPM}}{\sqrt{\text{Nm}}}$.

Examples of characteristic curves of a torque converter are shown in Fig. 2.9. The map can be replaced by an analytical model, the Kotwicki model [6], based on curve fitting.

2.4.3 Gear Ratios and Mechanical Gearbox

Gearings are purely mechanical components, with no control, that change the speed and torque transmitted between two shafts without altering the power flow. In practice, however, losses due to friction occur and reduce the output power with respect to the input power.

The simplest model for a gearing only accounts for the speed and torque ratios, without considering the losses due to friction. Indicating with the subscripts b and f the base and follower shaft (see Fig. 2.10), and with $g_{fb} = \frac{N_b}{N_f}$ the transmission ratio

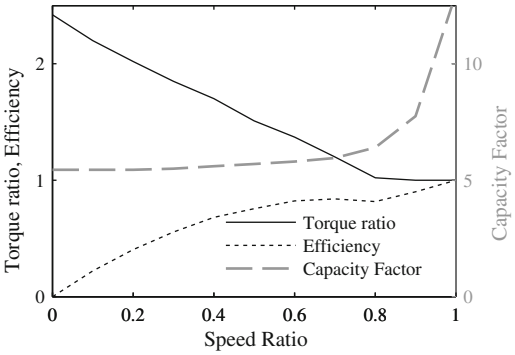

Fig. 2.9 Example of a torque converter map

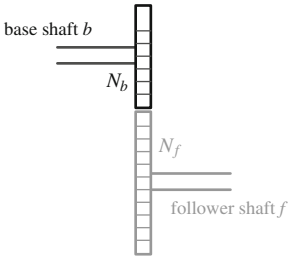

Fig. 2.10 Schematic representation of a gear coupling

(N is the number of teeth of each gear), the lossless gear model is:

$$\begin{cases} \omega_f = g_{fb}\omega_b, \\ T_f = \frac{1}{g_{fb}} T_b. \end{cases} \tag{2.17}$$

For energy analysis and in general for more accurate predictions, a lossy gear model is introduced, which takes into account power losses. Given that the speed ratio is fixed, being given by kinematic constraints, the speed equation remains the same as the lossless model, while the power loss means a reduction of the torque at the output shaft, described using the gear efficiency η_{fb}:

$$T_f = \begin{cases} \frac{\eta_{fb}}{g_{fb}} T_b & \text{if } P_b = T_b \cdot \omega_b \geq 0, \\ \frac{1}{\eta_{fb} \cdot g_{fb}} T_b & \text{if } P_b = T_b \cdot \omega_b < 0. \end{cases} \tag{2.18}$$

with the convention that power flow is positive when going from b to f, i.e., when b is the input shaft. The power loss is always positive and is calculated as

$$P_{loss} = \begin{cases} \omega_b T_b (1 - \eta_{fb}) & \text{if } P_b = T_b \cdot \omega_b \geq 0, \\ \omega_f T_f (1 - \eta_{fb}) & \text{if } P_b = T_b \cdot \omega_b < 0. \end{cases} \tag{2.19}$$

Functionally, a gearbox is a gearing whose transmission ratio (and possibly other characteristics, such as efficiency) can change dynamically. The simplest model for a gearbox consists in a lossy gear with variable gear ratio; the efficiency can be assumed constant or variable with gear ratio, speed, and input torque. This model captures the essential functionality common to manual gearboxes and automatic transmissions, and can be used for both cases. A complete transmission model with several degrees of freedom (considering all the gears, coupling and actuators) is more suited for drivability studies.

2.4.4 Planetary Gear Sets

Planetary gear sets are composed by three rotating elements (sun, carrier, and ring) which are connected by internal gears (planets); stopping one of the three shafts generates a fixed gear ratio between the remaining two. Planetary gears are commonly used in traditional automatic transmissions because they allow for compact construction and smooth gear transition. They are often present in hybrid electric vehicles to realize electrically variable transmissions (EVTs) by connecting the engine and two electric machines to the three shafts of the gear set.

A schematic representation of a planetary gear set is shown in Fig. 2.11.

The tangential speed of the carrier (at the center of the planets, i.e., at a radius intermediate between sun and ring) is the average of the sun and ring speeds. Indicating with the subscripts s, r, and c the sun, ring, and carrier shafts, the following kinematic constraint can be written:

$$\omega_c(N_r + N_s) = (\omega_r N_r + \omega_s N_s)\,, \tag{2.20}$$

where N_r and N_s are the number of teeth of the ring and sun gear, respectively. The reason for writing this relation in terms of number of teeth instead of radii is that—in a given gear set—the number of teeth N of each gear is directly proportional to the radius of the respective gear.

Introducing the planetary gear ratio $\rho = N_s/N_r$ (the ratio of the number of teeth of sun to the number of teeth of the ring), the kinematic relation (2.20) is written in

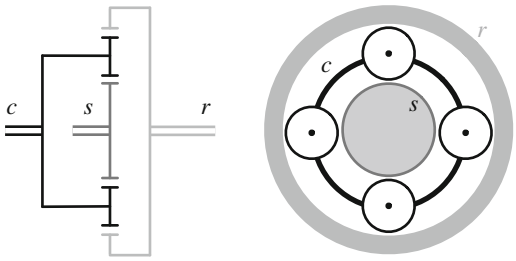

Fig. 2.11 Schematic representation of planetary gear set

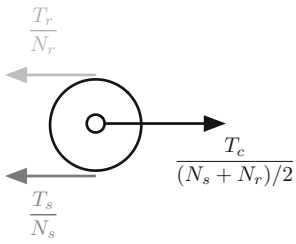

Fig. 2.12 Torque balance on the planets

the more compact form:

$$(1+\rho)\omega_c = \rho\omega_s + \omega_r. \tag{2.21}$$

The torque at the carrier at steady state is equally split between the sun and the ring; for the equilibrium of the planets (Fig. 2.12), the following torque equations hold:

$$\frac{T_c}{(N_r+N_s)} = \frac{T_r}{N_r}, \tag{2.22a}$$

$$\frac{T_c}{(N_r+N_s)} = \frac{T_s}{N_s}, \tag{2.22b}$$

where, again, the number of teeth are used instead of the radii. Using the planetary gear ratio $\rho = N_s/N_r$, the equilibrium equations become:

$$T_c = (1+\rho)T_r, \tag{2.23a}$$

$$T_s = \rho T_r. \tag{2.23b}$$

Equations (2.21) and (2.23a, 2.23b) are the basis for modeling planetary gear sets. The torque equations (2.23a, 2.23b) are only valid in steady-state conditions and neglect losses, but can be used with reasonable accuracy in vehicle-level models.

2.4.5 Wheels, Brakes, and Tires

The wheel represents the link between the powertrain and the external environment. Its model includes the motion of the wheel and the effect of the brakes, calculating the forces at the interface between tire and road surface. The tractive force is calculated given the powertrain torque, the brake signal and the vertical load on the wheel. A quasi-static model is usually sufficient, while dynamic tire models (see, for example, [4]) are typically used in models for vehicle lateral dynamics (handling models).

The static tire model could be defined a *perfect rolling* model, in which the torque applied to the wheel shaft is completely transformed into tractive force considering

pure rolling motion between the tire and the road, and neglecting tire deformation. These hypotheses work well for driving in normal conditions (not extreme accelerations) on roads with good adherence (dry asphalt). Low-adherence roads or extreme maneuvers require more accurate tire models to predict vehicle behavior in terms of speed dynamics.

The brakes can be modeled as an additional torque that reduces the net torque acting on the tire. The brake torque is proportional to the brake input signal. Therefore the net tractive force acting on the wheels is

$$F_{trac} = \frac{1}{R_{wh}} \cdot \left(T_{pwt} - T_{brake}\right) \tag{2.24}$$

where T_{pwt} is the torque generated by the powertrain at the wheel shaft, T_{brake} the braking torque, and R_{wh} the wheel radius.

The wheel speed is

$$\omega_{wh} = \frac{v_{veh}}{R_{wh}}, \tag{2.25}$$

being v_{veh} the longitudinal vehicle speed.

The value of longitudinal force is bounded by the vertical load acting on the wheel:

$$-F_z \nu_{x,max} \leq F_{trac} \leq F_z \nu_{x,max}, \tag{2.26}$$

where F_z is the vertical force on the wheel, and $\nu_{x,max}$ is the peak value of the road/tire friction coefficient (usually around 0.8–0.9 for dry asphalt). In order to maintain proper vehicle stability and maximize braking efficiency, the braking action must be distributed between front and rear axles according to the normal load acting on each, also accounting for the longitudinal load transfer generated by the deceleration. From (2.1), the total tractive force during braking is:

$$F_{trac} = M_{veh}\dot{v}_{veh} + F_{roll} + F_{aero} + F_{grade}. \tag{2.27}$$

This should be distributed between the front and rear axle (f and r) proportionally to the vertical load on each, i.e.:

$$\frac{F_{trac,f}}{F_{trac}} = \frac{b}{a+b} - \frac{M_{veh}\dot{v}_{veh}h_{CG}}{M_{veh}g(a+b)} \tag{2.28}$$

$$\frac{F_{trac,r}}{F_{trac}} = \frac{a}{a+b} + \frac{M_{veh}\dot{v}_{veh}h_{CG}}{M_{veh}g(a+b)} \tag{2.29}$$

where a and b are the distances of the center of gravity (CG) from the front and rear axle respectively, and h_{CG} its height from the ground. The terms that include the acceleration $\dot{v}_{veh}$ represent the dynamic load transfer, from the rear axle to the front axle during deceleration (negative $\dot{v}_{veh}$), and in the opposite direction during

acceleration. In most passenger vehicles, the powertrain generates torque only on one of the two axles. In that case, regenerative braking can only be applied to that axle, and must be appropriately balanced by conventional braking on the other axle. From the energy management standpoint, this means that not all the braking torque can be regenerated, but only the fraction of it that is applied at the traction axle, i.e., (2.28) for front-wheel drive or (2.29) for rear-wheel drive vehicles.

2.4.6 Electric Machines

The electric machines can be modeled using an approach similar to the one used for the engine, i.e., based on maps of torque and efficiency. Desired values of electrical power or torque can be used as a control input. Rotor inertia is the main dynamic element that is usually modeled, as the electrical dynamics are very fast in comparison with the inertial dynamics or the engine dynamics.

The relation between torque at the shaft and electric power is provided by an efficiency map, which can be expressed as a function of speed and torque, or speed and electrical power (depending on the implementation).

The efficiency map can also include the power electronics between the main electric bus and the machine to provide directly the electric power exchanged with the battery; otherwise, an explicit power electronics efficiency should be included in the model between the electric machine and the battery.

The efficiency model can be expressed as,

$$P_{mech} = \omega_{em} \cdot T_{em} = \begin{cases} \eta_{em}(\omega_{em}, P_{elec}) \cdot P_{elec} & \text{if } P_{elec} \geq 0 \text{ (motoring mode)}, \\ \frac{1}{\eta_{em}(\omega_{em}, P_{elec})} P_{elec} & \text{if } P_{elec} < 0 \text{ (generating mode)}, \end{cases} \tag{2.30}$$

or, if electric power is the desired output, as

$$P_{elec} = \begin{cases} \frac{1}{\eta(\omega_{em}, T_{em})} P_{mech} = \frac{1}{\eta_{em}(\omega_{em}, T_{em})} \omega \cdot T_{em} & \text{if } P_{elec} \geq 0 \text{ (motoring mode)}, \\ \eta_{em}(\omega_{em}, T) \cdot P_{mech} = \eta_{em}(\omega_{em}, T_{em}) \cdot \omega_{em} \cdot T_{em} & \text{if } P_{elec} < 0 \text{ (generating mode)}. \end{cases} \tag{2.31}$$

An example of efficiency map for an electric motor is shown in Fig. 2.13.

2.4.7 Batteries

Electrochemical energy storage systems such as batteries and capacitors are key components of hybrid electric vehicles. A variety of models have been proposed to evaluate their interaction with the rest of the powertrain [8].

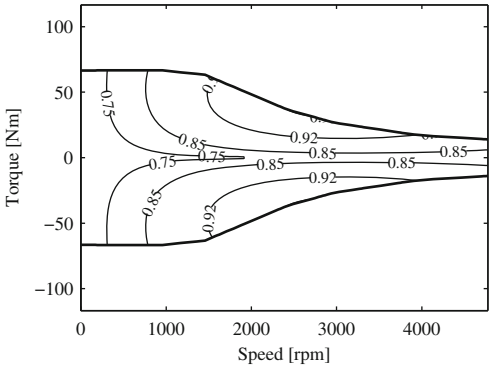

Fig. 2.13 Example of electric motor efficiency map (elaboration of data in [7])

Accurately modeling battery dynamics in hybrid electric vehicles is critical and not trivial, because the main variables that characterize battery operation, i.e. state of charge, voltage, current and temperature, are dynamically related to each other in a highly nonlinear fashion. In general, the objective of the battery model in a vehicle simulator is to predict the change in state of charge given the electrical load.

The state of charge (SOC) is defined as the amount of electrical charge stored in the battery, relative to the total charge capacity:

$$SOC(t) = \frac{Q(t)}{Q_{nom}}, \tag{2.32}$$

where Q_{nom} is the nominal charge capacity, and $Q(t)$ the amount of charge currently stored. The SOC dynamics are given by:

$$\dot{SOC}(t) = \begin{cases} -\frac{1}{\eta_{coul}} \frac{I(t)}{Q_{nom}} & \text{if } I(t) > 0 \\ -\eta_{coul} \frac{I(t)}{Q_{nom}} & \text{if } I(t) < 0 \end{cases} \tag{2.33}$$

where I is the battery current (positive during discharge), η_{coul} is the Coulombic efficiency [1] or charge efficiency, which accounts for charge losses and depends on current operating conditions (mainly current intensity and temperature).

Calculating the state of charge (or, better, its variation) by integration of (2.33) appears to be relatively straightforward, if the capacity is assumed to be a constant, known parameter. In reality, the battery capacity and coulombic efficiency change according to several parameters, and the numerical integration is reliable only in simulation in the absence of measurement error and noise, which makes reliable state of charge estimation a significant portion of the actual battery management system (BMS) [8].

In order to correlate the battery current and voltage to the power exchanged with the rest of the powertrain, a circuit model of the battery can be used.

A simple dynamic model is a circuit like the one in Fig. 2.14, which represents a second-order approximation.

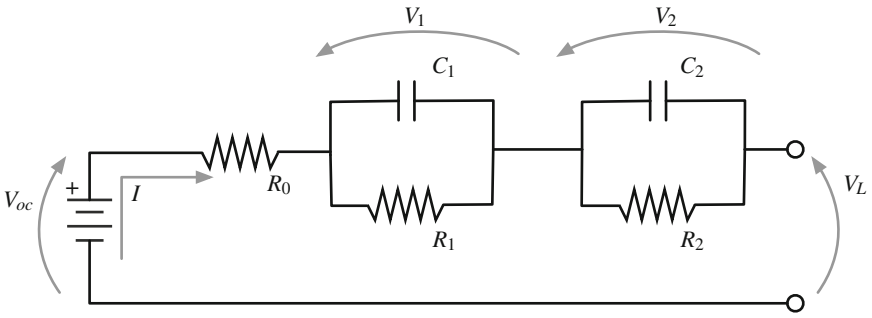

Fig. 2.14 Battery equivalent circuit-based model (second-order)

Fig. 2.15 Battery circuit model (no dynamics)

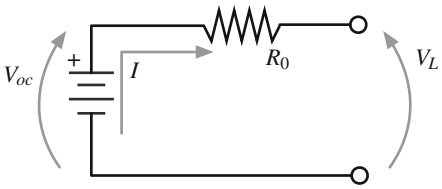

The series resistance R_0 represents the Ohmic losses due to actual resistance of the wires and the electrodes and also to the dissipative phenomena that reduce the net power available at the terminals; the resistances R_1, R_2 and the capacitances C_1, C_2 are used to model the dynamic response of the battery. The values of the parameters are estimated using curve fitting of experimental data, and are generally variable with the operating conditions (temperature, state of charge, current directionality). Other models of the same kind, with more or fewer R–C branches in series, can be used depending on the required model accuracy. However, the number of parameters to be identified increases with the model order. Very often, simpler models without any R–C branch (Fig. 2.15) can also be used if the voltage dynamics can be neglected, for example in quasi-static models focusing exclusively on efficiency considerations. When no detailed data from battery testing is available, circuit models with a single, constant R_0 may be the only option.

The equations of the circuit in Fig. 2.14 are:

$$V_L = V_{oc} - R_0 I - \sum_{i=1}^{n} V_i, \tag{2.34}$$

$$C_i \frac{dV_i}{dt} = I - \frac{V_i}{R_i}, \tag{2.35}$$

where V_L is the load voltage at the battery terminals, V_{oc} is the open circuit voltage, i.e., the voltage of the battery when it is not connected to any load ($I = 0$), R_0 the series resistance, V_i the voltage across the ith R–C branch (characterized by the resistance

R_i and the capacitance C_i), n is the order of the dynamic model considered, i.e., the number of R–C branches. In the example shown, $n = 2$. The capacitance C_i and the resistance R_i can change with the direction (charge or discharge) and amplitude of the current and with other operating conditions, such as temperature and state of charge; the variation can be taken into account by expressing the parameters as maps (tables) instead of constants.

If voltage dynamics are neglected and the battery circuit is represented without R–C branches as in Fig. 2.15, the circuit equation is easily written as a function of the terminal power P_{batt}:

$$P_{batt} = V_L \cdot I = V_{oc} I - R_0 I^2, \tag{2.36}$$

thus providing an explicit expression of the current as a function of power:

$$I = \frac{V_{oc}}{2R_0} - \sqrt{\left(\frac{V_{oc}}{2R_0}\right)^2 - \frac{P_{batt}}{R_0}}. \tag{2.37}$$

The circuit representation of Figs. 2.14 and 2.15 and the corresponding equations are referred to the entire battery pack. This is usually composed by many cells connected in series (strings), and possibly several strings in parallels. The electrical parameters of the circuit models are those of the entire pack, which can be computed from the values of each cell as follows:

$$V_{oc} = N_S V_{oc,cell}, \tag{2.38}$$

$$R_i = \frac{N_S}{N_P} R_{i,cell}, \quad i = 0, \ldots, n \tag{2.39}$$

$$C_i = \frac{N_P}{N_S} C_{i,cell}, \quad i = 1, \ldots, n \tag{2.40}$$

where N_S is the number of cells in series in each string, and N_P is the number of strings in parallel.[4]

The open circuit voltage V_{oc} is a typical characteristic of the battery (or, better, of its cells) and is primarily a function of the state of charge. An example of variation of the open circuit voltage V_{oc} with the state of charge for a single Li-Ion cell is shown in Fig. 2.16. The figure also shows the internal resistance of the same cell. It is common practice to refer to the value of the current in terms of its C-rate, i.e., as a fraction of the battery capacity (expressed in Ah): for example, if the capacity is 6.5 Ah, a current of 1 C corresponds to 6.5 A, 10 C–65 A, 0.1 C–0.65 A. Steady-state characteristics of the battery, such as those of Fig. 2.16, are typically obtained using a current of 1 C.

[4] Equations (2.38)–(2.40) are simplifications based on the assumption of ideal cells, all identical. In reality, each cell may have slightly different characteristics, for manufacturing issues and for normal imbalance during operation.

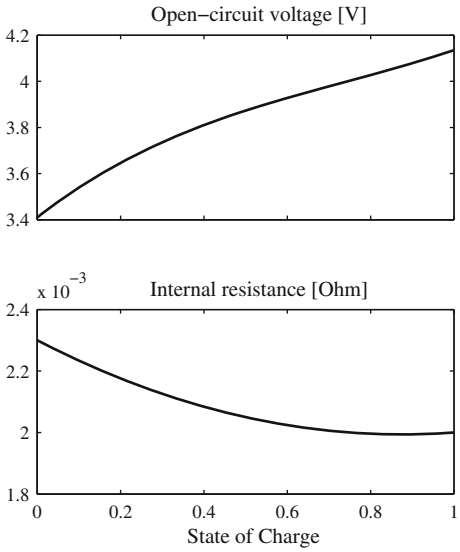

Fig. 2.16 Typical characteristics of open circuit voltage and internal resistance for a Li-Ion cell (Data referred to one blended cathode composed of layered-oxide positive electrodes and spinel oxide positive electrodes pouch Li-Ion cell, obtained from experiments at the Center for Automotive Research—The Ohio State University)

Apparently, integration of the current is sufficient to calculate the state of charge; however, in real-world applications, this is not stable (for numerical drift) nor accurate (for modeling approximations); therefore, more complex *SOC* estimation algorithms are used, which provide an estimate of the battery state of charge given available measurements of terminal voltage and current.

An important issue related to battery usage in hybrid electric vehicles is their aging, due to the aggressive loading cycles to which they are subjected. Battery aging manifests itself as loss of capacity and increase of internal resistance and can reduce vehicle performance; recent and ongoing research is devoted to determine a suitable model that can predict the amount of residual life given the loading cycles [9–13].

The dependence on aging does not affect battery performance in the short term and is only apparent over a long period of time, that exceeds any typical powertrain/vehicle simulation horizon; therefore, it is not taken into account as a dynamic effect in this study.

2.4.8 Engine Accessories and Auxiliary Loads

The engine powers several auxiliaries, such as air conditioning, power steering, alternator for small electric loads, etc. A simplified modeling approach is often used, for the lack of detailed data and load cycles for all the components, using the net power as an input in the form of a load cycle, and computing the torque as the ratio

of power to speed, including an efficiency computed using a look-up table, curve fitting, or constant value (depending on the case).

Auxiliary loads are important especially in heavy-duty vehicles with specialized use, but may be significant also in passenger vehicles. For example, the power demand of the air-conditioning system in a compact car can be as high as 10 % of the maximum engine power. Due to the great variety of possible auxiliary loads in a vehicle, an attempt to first-principle modeling cannot be generalized and must be derived for the specific application. For this reason, instead of dealing with detailed modeling of the accessories, the usual approach is to assume a known torque or power profile generated by the auxiliary loads at the engine shaft (if they are mechanically driven), or electric power at the bus interface (if they are electrically powered). In many cases, especially for passenger cars, the auxiliary loads are assumed to be constant for the entire driving cycle, using an estimate average value, whose order of magnitude is 1–4 kW.

References

1. L. Guzzella, A. Sciarretta, *Vehicle Propulsion Systems: Introduction to Modeling and Optimization* (Springer, Berlin, 2013)
2. L. Serrao, C. Hubert, G. Rizzoni, Dynamic modeling of heavy-duty hybrid electric vehicles, in *Proceedings of the 2007 ASME International Mechanical Engineering Congress and Exposition* (2007)
3. P. Sendur, J.L. Stein, H. Peng, L. Louca, An algorithm for the selection of physical system model order based on desired state accuracy and computational efficiency, in *Proceedings of the 2003 ASME International Mechanical Engineering Congress and Exposition*. Washington, DC, USA (2003)
4. H.B. Pacejka, *Tire and Vehicle Dynamics* (Butterworth-Heinemann, Oxford, 2012)
5. P. Pisu, C. Cantemir, N. Dembski, G. Rizzoni, L. Serrao, J. Josephson, J. Russell, Evaluation of powertrain solutions for future tactical truck vehicle systems, in *Proceedings of SPIE*, vol. 6228 (2006)
6. A.J. Kotwicki, Dynamic models for torque converter equipped vehicles. SAE Technical Paper No. 820393 (1982)
7. T.A. Burress, S.L. Campbell, C.L. Coomer, C.W. Ayers, A.A. Wereszczak, J.P. Cunningham, L.D. Marlino, L.E. Seiber, H.T. Lin, Evaluation of the 2010 Toyota Prius hybrid synergy drive system. Technical report, Oak Ridge National Laboratory (2011)
8. C.D. Rahn, C.-Y. Wang, *Battery Systems Engineering* (Wiley, Oxford, 2013)
9. S. Drouilhet, B. Johnson, A battery life prediction method for hybrid power applications, in *Proceedings of the 35th AIAA Aerospace Sciences Meeting and Exhibit*, Reno, NV (1997)
10. L. Serrao, Z. Chehab, Y. Guezennec, G. Rizzoni, An aging model of Ni-MH batteries for hybrid electric vehicles, in *Proceedings of the 2005 IEEE Vehicle Power and Propulsion Conference (VPP05)* (2005), pp. 78–85
11. Z. Chehab, L. Serrao, Y. Guezennec, G. Rizzoni, Aging characterization of Nickel—Metal Hydride batteries using electrochemical impedance spectroscopy, in *Proceedings of the 2006 ASME International Mechanical Engineering Congress and Exposition* (2006)
12. M. Dubarry, V. Svoboda, R. Hwu, B. Liaw, Capacity and power fading mechanism identification from a commercial cell evaluation. J. Power Sources **165**(2), 566–572 (2007)
13. M. Dubarry, V. Svoboda, R. Hwu, B. Liaw, Capacity loss in rechargeable lithium cells during cycle life testing: the importance of determining state-of-charge. J. Power Sources **174**(2), 1121–1125 (2007)

http://www.springer.com/978-1-4471-6779-2

Hybrid Electric Vehicles
Energy Management Strategies
Onori, S.; Serrao, L.; Rizzoni, G.
2016, XV, 112 p. 71 illus., 3 illus. in color. With online files/update., Softcover
ISBN: 978-1-4471-6779-2